HST DETECTION OF A QUIESCENT LOW MASS X-RAY BINARY COMPANION IN 47 TUCANAE [1]

PETER D. EDMONDS[2], CRAIG O. HEINKE[2], JONATHAN E. GRINDLAY[2] AND RONALD L. GILLILAND[3]

Accepted for publication by The Astrophysical Journal Letters

ABSTRACT

We present the results of a search for optical counterparts to the two quiescent low mass X-ray binaries (X5 and X7) in the globular cluster 47 Tucanae, using high quality *Chandra* and *HST* images. A faint blue ($V = 21.7$; $U - V = 0.9$) star within $0.''03$ of the eclipsing system X5 shows variability on both short and long timescales, and is the counterpart of the X-ray source. The colors and variability of this object are consistent with the combination of light from an accretion disk and a red main sequence star (possibly somewhat larger than a normal MS star with similar luminosity). No evidence is found for a star showing either variability or unusual colors near the position of X7, but a probable chance superposition of a star with $V = 20.25$ limits the depth of our search.

Subject headings: binaries: general – globular clusters: individual (47 Tucanae) – techniques: photometric –
X-rays: binaries

1. INTRODUCTION

It has long been thought that quiescent low mass X-ray binaries (qLMXBs) dominate the most luminous of the dim sources in globular clusters (Hertz & Grindlay 1983, Verbunt et al. 1984). Recent observations using Chandra/ACIS imaging and spectroscopy have demonstrated that this is indeed the case. Two systems, X5 and X7 in the massive globular cluster 47 Tuc were previously suspected to be qLMXBs (Hasinger, Johnston & Verbunt 1994, Verbunt & Hasinger 1998) but the sensitivity and resolution of *Chandra* was required to confirm this suspicion (Grindlay et al. 2001a, hereafter GHE01a and Heinke et al. 2001a, in preparation, hereafter HGL01). One qLMXB has also been found in each of NGC 6397 (Grindlay et al. 2001b; hereafter GHE01b) and ω Cen (Rutledge et al. 2001). These 4 qLMXB systems all have thermal spectra that are well modeled by hydrogen atmospheres of hot neutron stars (NSs), with no power law components required. None of them are obviously variable with the exception of X5 (HGL01) which shows deep eclipses as well as dips showing increased neutral hydrogen (X7 shows marginal evidence for a 5.5 hr period).

The logical extension of this work is to search for optical counterparts to these sources, using the potent combination of *Chandra* and *HST*. With astrometric errors $< 0.''1$ routinely being achieved for X-ray sources, optical identifications are being reported with unprecedented frequency. These identifications include cataclysmic variables (CVs) and BY Draconis variables (GHE01a, GHE01b), millisecond pulsars (MSPs; Edmonds et al. 2001, hereafter EGH01 and Ferraro et al. 2001) and active LMXBs (Heinke et al. 2001b and White & Angelini 2001).

Searches for optical counterparts to qLMXBs have been less successful. No counterpart has been found for the NGC 6397 qLMXB (any possible companion has $M_V > 11$; GHE01b) while the ω Cen qLMXB lies outside the field of view (FOV) of current *HST* datasets and stellar crowding will limit deep searches from the ground. Here, we report the use of high quality *Chandra* and *HST* data to search for optical counterparts to the 47 Tuc qLMXBs X5 and X7. We have discovered a faint, blue and variable counterpart to the eclipsing X5, as reported briefly in GHE01a. This detection, combined with the well determined period, distance, inclination and X-ray spectrum of X5 makes this the best constrained qLMXB known. We also report limits on the qLMXB X7. The astrometry, photometry and time series for both of these searches are described below.

2. OBSERVATIONS AND ANALYSIS

Details of the *Chandra* data used here are given by GHE01a and HGL01. The qLMXBs X5 and X7 have 4576 and 5488 counts respectively (over the 72 ksec observation), with internal, 1σ errors of $0.''0082$ and $0.''0089$ respectively. To search for optical counterparts to X5 and X7, two *HST* datasets have been analysed, the 8.3 d observations of Gilliland et al. 2000 (GO-8267: July 3 1999 to July 11 1999) and the archival data of Meylan obtained in three different epochs with ~ 2 year spacings (GO-5912: October 25 1995; GO-6467: November 3 1997; GO-7503: October 28 1999). The Gilliland data provides exquisite V and I time series (with some U data) and the Meylan data provides F300W images in the first two epochs and F300W and F555W images in the third epoch (with limited time series information in each epoch).

2.1. *Astrometry*

Using the zeropoint positional offsets between the *Chandra* and *HST* coordinate frames, the region within $\sim 2.''0$ of the nominal X5 position lies outside the FOV of the Gilliland data set, but is found on the inner part (with respect to cluster center) of the WF4 chip in the Meylan data. Since no *Chandra* source in the WF4 FOV with > 50 counts (not including X5) currently has a plausible optical counterpart, we used the PC astrometry to align the X-ray and optical coordinate frames (incurring a systematic chip-to-chip error, assumed to be $0.''05$, which dominates the total error budget). After this correction we found that only three stars are within $0.''5$ of the nominal X5 position, with separations of $0.''033$ (0.6σ; C1), $0.''23$ (4.5σ; C2) and $0.''292$ (5.7σ; C3). The finding chart shows the F300W (Fig. 1a) and F555W (Fig. 1b) images, from Meylan epoch 3, for the region around X5 and the insets in Fig. 1a show epochs 1 ('U(1)') and 2 ('U(2)'). Since faint red MS stars appear brighter in the

[2] Harvard-Smithsonian Center for Astrophysics, 60 Garden St, Cambridge, MA 02138; pedmonds@cfa.harvard.edu; cheinke@cfa.harvard.edu, josh@cfa.harvard.edu

[3] Space Telescope Science Institute, 3700 San Martin Drive, Baltimore, MD 21218; gillil@stsci.edu

F555W image than in the F300W image, Figures 1a and 1b show that C1 has a blue color. However, C3 (just outside the 5σ error circle to the NE) has an even stronger blue color and so is also a potentially viable optical counterpart if the astrometric shift between the PC and WF4 chips is much larger than assumed. This ambiguity is resolved by noting that C1, unlike C3, is clearly brighter in epoch 1 than in epoch 2 (see inset) confirming it as the optical counterpart (hereafter $X5_{opt}$).
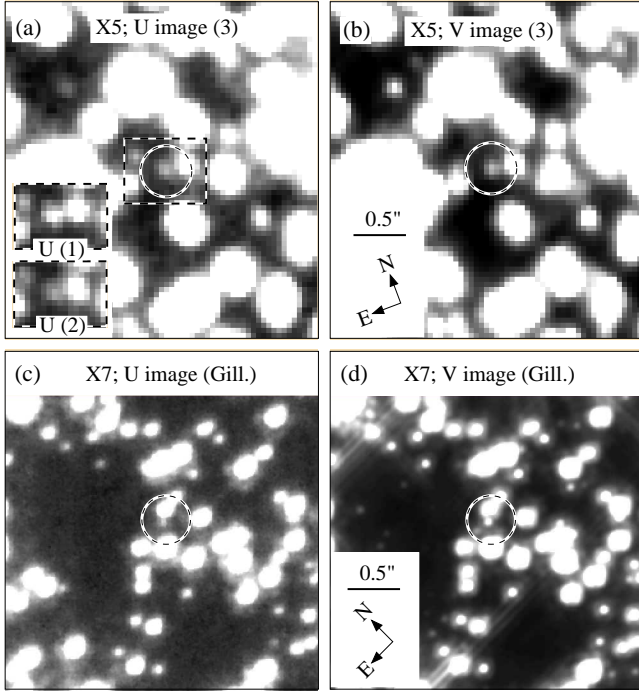

FIG. 1.— Finding charts for X5 and X7. For X5 the 3rd epoch combined F300W ('U'; Fig. 1a) and F555W ('V'; Fig. 1b) images are shown. The X5 companion ($X5_{opt}$) is near the center of the 5σ error circle, and the inset shows the area around $X5_{opt}$ from the 1st and 2nd epochs (note the clear variability of $X5_{opt}$). For X7 the deep, oversampled combined F336W ('U'; Fig. 1c) and F555W ('V'; Fig. 1d) images from Gilliland et al. (2000) are shown. The star N1 is found near the center of the 20σ error circle.

The region within a few arcsec of X7 falls on the PC images of both the Gilliland and Meylan data sets. Since 17 *Chandra* sources have likely optical counterparts on the Gilliland PC image, we have corrected for small linear terms in the residual astrometric errors between *Chandra* and *HST* using least squares fitting. We computed the positional errors for X7 by adding the systematic errors to the random `wavdetect` errors in quadrature, resulting in 1σ errors of $0\rlap{.}''0065$ in RA and $0\rlap{.}''0088$ in Dec (see Fig. 1c and 1d, where 20σ error circles are shown). The three nearest stars to X7 in the Gilliland *HST* image are $0\rlap{.}''019$ (2.3σ), $0\rlap{.}''12$ (14.7σ) and $0\rlap{.}''23$ (28.6σ) away (N1, N2 and N3 respectively). Clearly, astrometrically, only N1 ($V = 20.25$; $U-V = 1.72$; $M_V = 6.8$) is a viable candidate for the optical companion of X7. Given the FOV of the PC and the detected number of stars on the PC chip with $V < 20.25$ (6367), only 6.3×10^{-3} stars are expected within $0\rlap{.}''019$ of N1, assuming constant density over the PC FOV.

2.2. *Photometry*

The Gilliland dataset photometry (containing only X7) is described in Gilliland et al. (2000) and Albrow et al. (2001). The photometry for the Meylan observations (containing X5 and X7) was based on combining the images at each epoch using drizzle routines (Hook, Pirzkal, & Fruchter 1999) in STSDAS and then using PSF-fitting in DAOPHOT to calculate instrumental magnitudes. The F555W filter is a good approximation to Johnson V (Holtzman et al. 1995), but F300W differs significantly from the nearest Johnson filter (U). Therefore, we used ground-based photometry of 47 Tuc (Sills et al. 2000) and matching of main sequence (MS) turnoffs between the *HST* and ground-based datasets to calculate the zeropoint and then applied corrections to F300W-V (by measuring MS ridgelines) to convert it to $U-V$. By definition this MS-ridgeline technique is only applied to stars (like $X5_{opt}$) with colors ranging from the main sequence turn-off to the detected end of the MS.
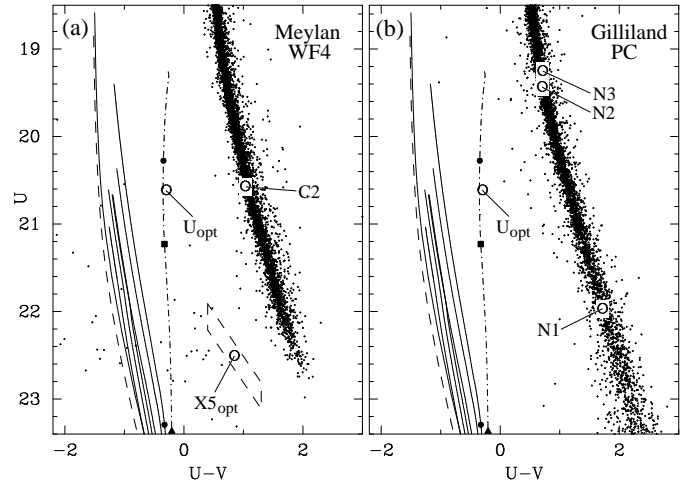

FIG. 2.— U vs $U-V$ CMDs for the Meylan WF4 chip (containing $X5_{opt}$; Fig. 2a) and the Gilliland PC chip (containing X7; Fig. 2b). For $X5_{opt}$ we show ranges in magnitude and color given limits on the variability. Near neighbors to $X5_{opt}$ and X7 are shown (apart from C3 which is not detected in the F555W image. Also shown are CO WD cooling sequences from Bergeron, Wesemael & Beauchamp (1995; thick lines) and He WD cooling sequences from Serenelli et al. (2001; thin lines). The dot-dashed sequence is the lowest mass model (the MSP counterpart U_{opt} from EGH01 is also shown).

Since this technique is non-standard we have performed two consistency checks with other calibration methods. We applied this technique to the Meylan PC data and performed a star-by-star comparison between our photometry and the Gilliland et al. (2000) photometry. Mean differences between the two photometric systems were < 0.05 mag in both U and V. A star-by-star comparison between the MS-ridgeline V calibration for the Meylan WF4 chip (containing $X5_{opt}$) and the standard calibration of Holtzman et al. (1995) applied to a 47 Tuc F555W image from the archive (program GO-6095), also gave mean errors < 0.05 mag. Combined with the 0.1 mag rms internal error in $U-V$ at the U mag of $X5_{opt}$, we estimate absolute errors for $X5_{opt}$ of ~ 0.2 mag in both U and V.

The color magnitude diagrams (CMDs) for the Gilliland PC and Meylan WF4 images are shown in Fig. 2. Fig. 2a shows the mean epoch 3 CMD position of $X5_{opt}$ ($V = 21.7$; $U-V = 0.9$; $M_V = 8.2$), along with reasonable ranges in magnitude and color given the variability (see below). With $M_V = 8.2$, $X5_{opt}$ has a similar absolute magnitude to that of the qLMXBs Cen-X4 ($M_V = 7.5 - 8.5$; Chevalier et al. 1989) and Aql X-1 ($M_V = 8.1$; Chevalier et al. 1999). Also shown are CO and He WD cooling sequences (see caption). Clearly, $X5_{opt}$ is unlikely to be either a CO WD or a He WD, unlike the MSP companion U_{opt}

(EGH01). Instead, it is more likely that the CMD position of $X5_{opt}$ represents the sum of a red MS star and a blue component from an accretion disk (see below).
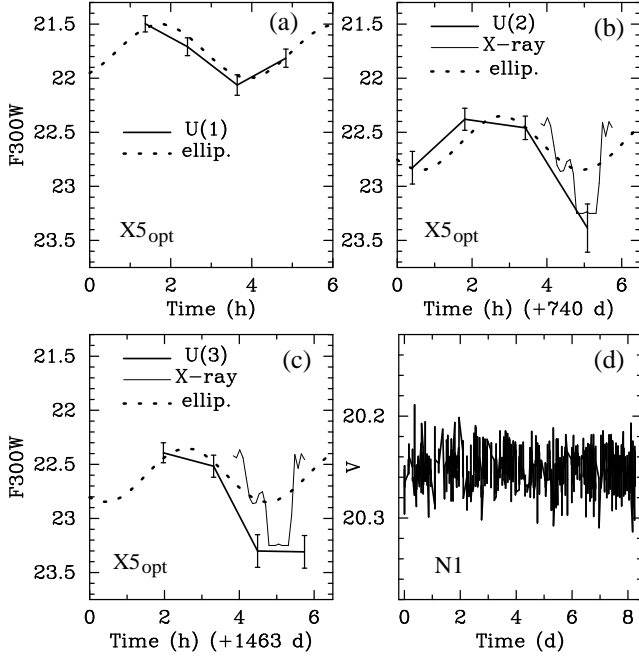

FIG. 3.— F300W time series for $X5_{opt}$ for epochs 1, 2 and 3 (Figures 3a, b and c respectively) with time offsets between epochs as shown. For $X5_{opt}$ a simple ellipsoidal model ('ellip.'), eclipse not included, is shown (zeropoints adjusted to the data). Also shown is the eclipsed portion of the X-ray phase plot (units converted into time) from HGL01. The 1σ error bars are the median time series rms for stars within 0.25 mag of a given magnitude level. Figure 3d shows the V-band time series for N1, the nearest possible counterpart to X7.

Fig. 2b shows the Gilliland CMD for X7 showing the position of the three nearest stars (N1, N2 and N3). The only viable counterpart astrometrically, N1, falls very close to the MS ridge line (also in V vs $V-I$) and therefore appears like a normal MS star (unlike $X5_{opt}$). This CMD position is consistent, within the errors, with the position in the Meylan data, and the F300W magnitudes from the three epochs are consistent with non-variability, again unlike $X5_{opt}$. This suggests that N1 is probably not the X7 counterpart, despite the good astrometric match. Assuming that the real counterpart falls in the less confused part of a 5-σ error circle we set limits on its detection of $U > 23$, $V > 23$, $I > 22$ (using the Gilliland data).

2.3. *Time Series*

Since $X5_{opt}$ is near (or beyond) the limit of detectability in individual F300W exposures, the time series for $X5_{opt}$ were calculated by co-adding groups of 3-4 images. Figures 3a, b and c show the F300W time series for the 3 different epochs. Also shown are the eclipsed portion of the X-ray phase plot from HGL01 (units converted into time) and a 4.333 hour period sinusoid, as appropriate for X5 but with the 8.666 hour X-ray period divided by two to simulate a double-peaked (ellipsoidal) time series. Eclipses are not included in this model. This model has been shifted in time and magnitude so that it plausibly matches the data for each epoch (the period is not known with sufficient accuracy to phase correct from *Chandra* to different *HST* epochs). Significant variability is seen within all three epochs and $X5_{opt}$ is clearly brighter in epoch 1 than in the 2nd and 3rd epochs (see Fig 1a). This longterm

variability is further evidence for the presence of an accretion disk. Note the deep eclipse observed in both epochs 2 and 3. The F300W eclipse appears to be significantly wider than in X-rays, though we do not observe the system coming out of eclipse. The turnover at the beginning of the second epoch (near Time= 0 hr) may represent a minimum from ellipsoidal variability, since the timescale of variability agrees well with the ellipsoidal model. The 1st epoch observations may also represent ellipsoidal variations rather than an eclipse, since in its brighter state the relative brightness of the disk compared to the secondary should be enhanced and the eclipse depth should increase. The V-band variations, not plotted here, show neither an eclipse nor clear evidence for ellipsoidal variations (expected to have a smaller amplitude than in F300W).

No suggestion of variability is present in the N1 time series (Fig. 3d) and no significant signal is seen in the N1 power spectrum (V or I), including the possible 5.5 hr period noted by HGL01. The highest peak in the V-band corresponds to a period of 2.52 hours (or twice this), with a false-alarm probability $= 0.27$. The corresponding V amplitude is 0.0043 ± 0.0011 (< 4-σ, insignificant for a blind search; similar results hold for I). If N1 *is* the X7 counterpart and is close to filling its Roche lobe then an inclination $< 2.5°$ is required to reduce the amplitude for ellipsoidal variations from the maximum expected value of ~ 0.1, for $90°$ inclination, to < 0.0043. This implies that N1 is unlikely to be the X7 companion, and we have calculated the brightness limit for a faint variable star (lying near the line of sight of N1) to be missed by our variability search. The X7 coordinates are so close to N1 that it will be included in any time series extraction. A star at $V = 22.9$ with intrinsic variations of 0.1 mag superimposed on the time series of N1 would yield an 8-σ detection (versus the highest detected peak at ~ 4-σ). This time series limit of $V \sim 23$ for a companion to X7 will decrease for inclinations $< 90°$.

3. DISCUSSION

Using the stellar models of Bergbusch & Vandenberg (1992), we estimated the brightest possible secondary consistent with our photometry ($T_{eff}= 4100$K, $V = 21.7$ and mass $= 0.53$M$_{\odot}$). Using the secondary radius, the X-ray luminosity of X5 and the binary separation (from Kepler's Third Law) we estimate that the maximum luminosity from heating of the secondary by the NS (when measured as a fraction of the secondary luminosity) is 2.7%. Therefore, secondary heating probably makes only a small contribution to the variability described above. The dominant sources of short-term variability are likely to be a combination of eclipses of the disk and hot spot by the MS star, ellipsoidal variations and flickering. Further observations are required to better define this variability.

The likely presence of an accretion disk in $X5_{opt}$, from variability and the blue color, may appear to be inconsistent with the lack of X-ray evidence for accretion currently in the X5 system, which should yield either long-term X-ray variations or a power law component, neither of which are seen (HGL01). One possible explanation is that the X5 secondary is no longer filling its Roche lobe causing it to be detached from the disk. Such a disk would no longer be accreting matter from the secondary, possibly causing it to enter a long-term quiescent phase with low density and little or no accretion onto the NS. The X5 disk does appear to be relatively faint compared to 47 Tuc CVs, since the $U-V$ color of $X5_{opt}$ (0.9) is much redder than that of

the 47 Tuc CVs V1, V2, W1 and W2 with $U-V$ colors ranging from -1.25 to -0.4 (Edmonds et al. 2001, in preparation).

To test this 'detached disk' theory we have estimated the degree to which X5$_{opt}$ fills its Roche-lobe as defined by F, the ratio between the stellar radius and the Roche lobe radius. Using the Roche-lobe formula from Paczyński (1971) ($r/a = 0.462[(M_{opt}/(M_{NS} + M_{opt})]^{1/3}$, where r is the Roche-lobe radius, a is the binary separation, M_{opt} is the mass of X5$_{opt}$, and $M_{NS} = 1.4M_\odot$), the stellar radius for a 4100 K model and the binary separation, we find that X5$_{opt}$ has $F = 0.6$, underfilling its Roche lobe. Fainter cooler secondaries will underfill their Roche lobes by slightly larger amounts (e.g. a star with $M_V = 10.0$ has $F = 0.5$). This behavior is consistent with the 'detached disk' theory given above, but would be inconsistent with the possible detection of ellipsoidal variations of relatively large amplitude, requiring the secondary to have $F \sim 1.0$. The latter possibility would suggest that the X5 secondary is either bloated or slightly evolved, as appears to be the case for some of the CVs in NGC 6397 (Grindlay et al. 2001, in preparation) and as might be expected for a star undergoing mass loss.

If the 5.5 hr X-ray period for X7 (HGL01) is real, and if the X7 secondary underfills its Roche lobe by about the same amount as X5$_{opt}$, then $M_V \sim 10.6$ and $V \sim 24.1$, beyond our variability detection limits and beyond our CMD search limit except with the presence of a reasonably bright disk. The close proximity of N1 only $\sim 0.''02$ from the line of sight of X7, clearly makes prospects for such an optical identification difficult. Alternatively, the period could be longer and N1 could be the counterpart, however the complete lack of evidence for a disk or variability rules against this possibility.

The logical follow-up to these observations are spectroscopic studies to measure the radial velocity amplitude of absorption lines from X5$_{opt}$. This, combined with the known inclination and spectroscopic and photometric determinations of M_{opt} would give an estimate of the mass of the X5 NS. Using the X-ray spectrum constraints on the NS radius and redshift (HGL01) combined with the NS mass would give the first compelling test of the equation of state of a NS. Also of interest would be the detection of emission lines in the optical spectrum. Since there is evidence for an accretion disk (from this work) and hot gas in the system (from the X-ray light curve), we expect strong disk or coronal emission lines to be superimposed on the absorption line spectrum of the secondary. Study of the emission line profiles can test for mass outflow (visible as P Cygni profiles) from the system, or detect evidence for a bipolar jet (visible as broadened emission lines).

REFERENCES

Albrow, M. D, Gilliland, R. L., Brown, T. M., Edmonds, P. D., Guhathakurta, P., & Sarajedini, A. 2001, ApJ, accepted

Bergbusch, P. A. & Vandenberg, D. A. 1992, ApJS, 81, 163

Bergeron, P., Wesemael, F., & Beauchamp, A. 1995, PASP, 107, 1047

Chevalier, C., Ilovaisky, S. A., van Paradijs, J., Pedersen, H., & van der Klis, M. 1989, A&A, 210, 114

Chevalier, C., Ilovaisky, S. A., Leisy, P., & Patat, F. 1999, A&A, 347, L51

Edmonds, P. D., Gilliland, R. L., Heinke, C. O., Grindlay, J. E., & Camilo, F. 2001, ApJ, 557, L57 (EGH01)

Ferraro, F. R., Possenti, A., D'Amico, N., & Sabbi, E. 2001, ApJ, submitted

Freire, P., Camilo, F., Lorimer, D. R., Lyne, A. G., Manchester, R. N. & D'Amico, N. 2000, MNRAS, In press (astro-ph/0103372)

Gilliland, R. L. et al. 2000, ApJ, 545, L47

Grindlay, J. E., Heinke, C. O., Edmonds, P. D. & Murray, S. 2001a, Science, 292, 2290 (GHE01a)

Grindlay, J. E., Heinke, C. O., Edmonds, P. D. Murray, S., & Cool, A. M. 2001b, ApJ, accepted (GHE01b)

Hasinger, G., Johnston, H. M., & Verbunt, F. 1994, A&A, 288, 466

Heinke, C. O., Edmonds, P. D. & Grindlay, J. E. 2001b, ApJ, accepted

Hook, R. N., Pirzkal, N., & Fruchter, A. S. 1999, ASP Conf. Ser. 172: Astronomical Data Analysis Software and Systems VIII, 8, 337

Hertz, P. & Grindlay, J. E. 1983, ApJ, 275, 105

Holtzman, J. A., Burrows, C. J., Casertano, S., Hester, J. J., Trauger, J. T., Watson, A. M., & Worthey, G. 1995, PASP, 107, 1065

Paczyński, B. 1971, ARA&A, 9, 183

Rutledge, R. E., Bildsten, L., Brown, E. F., Pavlov, G. G., & Zavlin, V. E. 2001, ApJ, submitted (astro-ph/0105405)

Serenelli, A. M., Althaus, L. G., Rohrmann R. D. & Benvenuto, O. G. 2001, MNRAS, 325, 607

Sills, A., Bailyn, C. D., Edmonds, P. D., & Gilliland, R. L. 2000, ApJ, 535, 298

Verbunt, F., Elson, R., & van Paradijs, J. 1984, MNRAS, 210, 899

Verbunt, F. & Hasinger, G. 1998, A&A, 336, 895

White, N. E. & Angelini, L. 2001, ApJ, accepted (astro-ph/0109359)

TABLE 1

POSITIONAL, PHOTOMETRIC AND TIME SERIES INFORMATION FOR X5$_{opt}$

qLMXB	RA[a] (J2000)	Dec[a] (J2000)	X[b]	Y[b]	U[c]	V[c]	period[d] (hours)
X5	00 24 00.991(1)	−72 04 53.202(7)	60.7	263.0	22.5(2)	21.7(2)	8.67
X7	00 24 03.528(1)	−72 04 51.938(6)	498.5	775.5	⋯	⋯	5.50

[a]Coordinates in MSP astrometric system; Freire et al. (2001)

[b]Pixel coordinates of X-ray sources using the STSDAS task METRIC applied to archival images u2ty0201t (X5) and u5jm070cr (X7)

[c]Epoch 3 mean magnitudes for X5$_{opt}$

[d]Periods from HGL01; value for X7 is from a marginal detection of variability